Modeling and microstructural analysis of temperature effects in fused silica viewport

M. Jacobs[a,c,*], G. Van Oost[a], J. Degrieck[b], I. De Baere[b], A. Gusarov[c], V. Massaut[c]
[a] Department of Applied Physics, Ghent University, Jozef Plateaustraat 22, 9000 Ghent, Belgium
[b] Department of Materials Science and Engineering, Ghent University, Sint-Pietersnieuwstraat 41, 9000 Ghent, Belgium
[c] SCK•CEN, Boeretang 200, 2400 Mol, Belgium

[*] Corresponding author. Tel.: +32 14 333473; E-mail: marijke.jacobs@sckcen.be, Address: SCK•CEN, Boeretang 200, 2400 Mol, Belgium

Abstract

In ITER glass-metal joints are necessary to seal the optical windows, which are installed on the vacuum vessel, in order to perform diagnostics. These joints have to resist temperatures in a range 150-200 °C during normal operation and 250-300 °C during vessel out-gassing, while keeping a good mechanical strength.
At the moment, there is a lack of data in literature about the behavior of glass-metal joints under ITER-relevant conditions. To obtain such data we studied the effect of temperature cycling on the microstructure of the glass-metal interface of a commercial brazed fused silica viewport. We have found that after thermal cycling already from RT to 100 °C cracks occurred in the interlayer (braze material) near the glass. With temperature increase the cracks became bigger and at 300 °C there was melting of one part of the interlayer, but the glass-metal joint sustained the treatment. To understand this behavior an elastic model of the viewport was developed using the Abaqus code. According to the model the temperature-induced maximum principal stresses in the interlayer exceeded the ultimate tensile strength of the braze alloy. The highest stresses in the interlayer were found near the glass, corresponding to the experimentally observed location of the cracks.

Keywords

Optical Viewport, Temperature Effects, Microstructure, Finite Element Modeling

1. Introduction

The ITER vacuum vessel will have a large number of windows, which are required for various plasma diagnostic systems [1]. In a number of windows silica will be used as the window material. As a part of the vacuum vessel, the windows must remain leak tight for the tritium and for protecting the vacuum. Other demands for the windows are being resistant against elevated temperatures and against neutron flux.
Most of currently fabricated commercial optical viewports are intended for the use in vacuum at temperatures up to 150-200 °C. Usually the glass has the coefficient of thermal expansion (CTE) similar to that of the metal part, so that thermally-induced stresses in the viewport create no significant problem. But those types of glasses are not suitable for the use in ITER because they contain impurities and therefore are very sensitive to ionizing radiation. High purity KU1 silica is now the most perspective candidate for ITER windows [2,3]. As fused silica has a very low CTE, thermal residual stresses arise in the joint when cooling down from the fabrication temperature. These stresses must be minimized as much as possible to have a strong joint. This is usually done by using a suitable brazing alloy.

The effect of ionizing radiation on the properties of optical windows was mainly studied in terms of their optical characteristics [2-5]. In contrast, to the best of our knowledge, there is very little information available on how these brazed viewports would behave under thermal cycling and under neutron irradiation relevant for the ITER operation. Zaccaria *et al.* [6] investigated the thermal and mechanical effects on glass for thermonuclear fusion experiments, but not on the total viewport. Only Lipa *et al*. [7] published some results about optical windows for ITER. They calculated thermo-mechanical stresses of sapphire windows for different heat loads and performed some tests on such windows according the ITER test specifications. The window assemblies passed the tests successfully without damage.
In the present work we performed thermal cycling tests on a brazed fused silica viewport and investigated the glass-metal interface with a scanning electron microscope (SEM). We also developed a finite element model using the code Abaqus/Standard ver. 6.9 to gain a better understanding of the distribution of the thermal stresses in the joint. Experimental and modeling results are compared with each other to allow a better understanding of the effects of temperature on the glass-metal joint of the optical viewport.

2. Samples and methods

2.1 Experimental samples

The fused silica viewport used in the study has a 304 stainless steel flange with the outer diameter of 70 mm and the 3.3 mm thick glass element, as illustrated in Figure 1. It is brazed with a lead-silver braze alloy (nominal composition 97.5 % Pb , 2.5 % Ag) that melts at 304 °C. Titanium is added to this braze alloy in order to improve the wetting. The mechanical properties of silica and 304SS can be found in standard handbooks [8] and are summarized in Table 1. For the braze alloy however, we did not have all the necessary data. After a mechanical property comparison of similar alloys, the use of the data of alloy 92.5Pb 5.0Sn 2.5Ag in Table 1 is justified [9].

We cut the viewport in several pieces using the waterjet cutting, so that the interface between the glass and the 304SS becomes assessable for the analysis. Waterjet cutting was used because it allows cutting through glass and metal at the same time. One of the samples is shown in Figure 2 with its dimensions. It can be seen that the transparent element is connected to the stainless steel viewport flange with a 0.3 mm thick holder membrane (Figure 2 right). One side of each sample was polished for investigation with the SEM. These samples were used to investigate the effect of the thermal cycling in different regimes on the glass-metal interface. Energy dispersive spectroscopy (EDS) was applied to determine the elemental composition in the interface.

2.2 Thermal cycling test

A first thermal cycling test included 4 cycles from 100 to 150 °C with a holding time of 20 minutes at the maximal temperature. It was done in vacuum at 4.5×10^{-3} mbar. The temperature was measured with a type K thermocouple placed in a close vicinity to the samples. We estimate the accuracy of the temperature measurements is ± 2.5 °C.
The cycling is considered to be relevant for the ITER operation. 150°C is the maximal acceptable operational temperature for the viewport and normally should not result in a failure. Nevertheless, after the test damage was already visible in the interface. To find out the temperature at which the damage starts to appear new cycling tests from RT up to 75 and 100 °C were performed on another sample, namely sample VP (Figure 2). Then thermal tests up to 200, 250 and 300 °C were also done on the same sample VP. Once there was damage observed after cycling at 100 °C, it was decided to do only one cycle to study the evolution of the damage under higher temperatures.

2.3 Finite element model

Finite element models (FEMs) were already used to study thermal stresses in brazed joints [10-13]. We applied the finite element software Abaqus/Standard ver. 6.9 to simulate the thermal stresses during our tests. The geometry and the meshing of the optical viewport model are given in Figure 3. The dimensions correspond to Figure 2: the length, width and thickness are 19, 17 and 3.2 mm, respectively. The thickness of the 304SS holder membrane attached to the silica element is 0.3 mm and the thickness of the brazing interlayer 0.850 mm. As there is a gap between the holder and the viewport flange (Figure 2 right), only the small width of 0.3 mm can be taken into account. In this model we started with a stress-free optical window at room temperature. Then the thermal stresses, created in the sample due to differences in the CTE upon heating to a desired temperature, were calculated. For this calculation a linear elastic model with the material properties from Table 1 and with cylindrical coordinates was used. Temperature-dependent material properties were not used as the modeling was only performed up to 200 °C. Meshing was done using hex-elements with a general size of 0.26 mm. Local seeds were used for the edges at the top and bottom of the viewport. There were 3 elements along the edge for 304SS and 11 elements for the braze layer. For the fused silica part near the braze layer a biased seed with a bias ratio of 3 and 50 elements was used. The other part of the fused silica and some edges of the 304SS have elements with a size of 0.5 mm. All these elements give a fine enough mesh. The calculations were also done with a rougher and a finer mesh, but the same conclusions can be drawn. So there is little mesh sensitivity. The stresses were mainly calculated along two paths, P1 and P2, from the 304SS to the glass. These paths are visualized in Figure 3.

3. Results and discussion

3.1 Microstructural effects of thermal cycling tests

The SEM picture shows that the glass-metal interface consists of two layers (Figure 4). With the EDS we see that only the interlayer 2 (next to the glass) contains titanium. Titanium is not dissolved but forms metallic particles, as it can be seen from Figure 5, thus making the interlayer brittle. The amount of Ti in this interlayer is around 27 %, which was determined by EDS. Interlayer 1 is just the Pb-Ag braze alloy with the Ag nicely spread out. The dark small spots in this interlayer are SiO_2 particles, which are descended from the waterjet cutting, so they are not a part of the viewport. They could penetrate interlayer 1, but not interlayer 2. This is because interlayer 2 is less soft than interlayer 1 thanks to the titanium. The particles are still present in the interface, because it is difficult to do a very profoundly manual polishing of the glass-metal interface. A part of the fused silica looks white because of the charging effect.

After each thermal cycling test, the interface of the sample VP was investigated with the SEM to study the effect of the temperature on the joint. The test up to 75 °C gave no detectable changes of the interface (Figure 6 B). Increase of the temperature up to 100 °C caused already small cracks in the interlayer 2 near the glass (Figure 6 C). The cracks were parallel to the glass-metal interface. With increasing the cycling temperature up to 250 °C, the cracks became more and more wide (Figure 6 D-E). However further temperature increase from 250 to 300 °C did not change the picture (Figure 5 F), probably because the stress is relieved due to the contact loss between the materials.
After the test at 100 °C also some small cracks in the glass came up (Figure 7 B), but not as much as in the interlayer 2. At 200 °C the cracks in the glass and in the interlayer 2 started to connect each other (Figure 7 C).
At the test temperature of 300 °C, which is close to the melting temperature of the braze alloy, melting indeed occurred, but only in the interlayer without Ti. Although interlayer 1 became

thinner, debonding of glass element did not occur. Figure 8 compares two pictures of the same part of the viewport with the same magnification after the thermal test up to 250 °C (A) and after the test up to 300 °C (B). After the 300°C test interlayer 1 of the interface has almost completely gone.

3.2 Analysis of thermal stresses

In order to know if there will occur any damage in the material by applying a thermal field, we used the failure analysis for brittle materials, namely 'the maximum principal stress theory'. According to this theory failure occurs when the largest principal stress exceeds the uniaxial tensile strength. As the modeling of the exact quantity of the metallic Ti pieces in the interlayer will cause very high localized stresses due to stress singularities, the effect of Ti must be investigated by another method. Therefore it was decided to model interlayer 2 of the braze layer in two different ways: with no titanium and with 100 % Ti. The real situation, 27 % Ti, will be somewhere between these two results. A uniform and non-uniform brazing layers create similar stresses in the rest of the sample, because the high local stress fields related with the Ti grains presence, decay within a short distance, which is small compared to the brazing layer thickness. As such, it is justified to model the braze layer with a uniform Ti layer.

In the first model, with no Ti, the maximum principal stress was calculated to look for possible damage in the viewport. Figure 9 shows the maximum principal stress for different temperatures along paths P1 and P2 (Figure 3) from the metal to the glass. The paths are situated at the side of the sample, because this is the same area that was analyzed with the SEM.

For all the temperatures the maximum principal stress is the highest in the glass near the braze layer. In the braze layer itself, there is a maximum in the middle. Between the braze layer and the glass, the values of the maximum principal stress are very different. At 75 °C the stress remains below 32 MPa everywhere in the glass. When the temperature is increased to 100 °C, the stress reaches a maximum of around 46 MPa. This is already close to the strength of fused silica, which is 50 MPa. With a temperature field of 150 °C the stress becomes almost 76 MPa, which is much higher than the strength of fused silica. So damage will certainly occur in the glass. For a temperature of 200 °C, the viewport is no longer useable. In the braze layer the maximum principal stress remains below 35 MPa up to temperature of 150 °C, so no damage should be expected in the braze layer according to this model.

In the second model, with a Ti layer, the maximum principal stress was again calculated along the same paths for a temperature increase up to 100 °C. The effect of the Ti is shown in Figure 10. If interlayer 2 consists out of fully Ti, there is a decrease of stress in the fused silica part. But in the Ti itself, the stress has become high. The stress profiles along paths P1 and P2 are more or less the same, except the high peak is shifted from the fused silica to the Ti layer. Now, the maximum principal stress exceeds the ultimate tensile strength of the braze alloy very much. Even if in reality the stress will be a bit smaller due to the smaller amount of Ti, damage can be expected in the braze layer. If the curve of 75 °C of Figure 9 is shifted to the braze layer, there will be no damage in the braze layer as the maximum principal stress reaches just the ultimate tensile strength of the braze alloy. So in reality, the maximum strength will not be obtained.

To see the general difference between the two models, the maximum principal stress for a temperature increase to 100 °C is plotted for the whole viewport in Figure 11 for each model. If the Ti is taken into account, the stress in the fused silica decreases, but in the braze layer near the glass it becomes much higher.

As the maximum principal stress exceeds the strength of the braze layer and reaches almost the strength of the fused silica at a temperature of 100 °C, there will certainly be damage in the

material. In order to know where the damage is situated in the material, it is important not only to look at the maximum principal stress, but also to examine each stress tensor component separately. The three principal stresses, calculated with the Ti model, are shown in Figure 12. Similar results were obtained with the other model. The stress in the radial direction, σ_{rr}, is the highest in the braze layer. So perpendicular to this direction, damage can occur. The stresses in the other directions are mainly high in the metal part and at the glass-braze interface. As the viewport consists out of different materials, shear stresses between the material layers can be expected when applying a temperature field. The shear stresses perpendicular to the radial direction, $\sigma_{r\theta}$ and σ_{rz}, are the highest at the borders of the braze-glass joint. As the fused silica is not so thick, $\sigma_{r\theta}$ will be more important than σ_{rz}. So only $\sigma_{r\theta}$, that will cause sliding between the fused silica and the braze layer, is shown in Figure 12. In case of the total viewport, the shear stress $\sigma_{r\theta}$ will not play a role anymore because of the axial symmetry of the viewport.

3.3 Discussion

As it was not possible to model exactly the viewport due to the Ti, two models were used to study the viewport. The modeling with both the models shows that at 75 °C the stresses in the viewport are all well below the values that lead to damage. So this temperature should not cause any damage in the viewport. This is in agreement with microstructural analysis results where no cracks were observed after a thermal cycling test up to 75 °C.
At 100 °C the maximum principal stress significantly exceeds the ultimate tensile strength in the interlayer close to the glass according to the Ti model. Furthermore, the highest shear stresses occurred along the braze-glass joint. This corresponds with the location where the cracks occurred after the thermal cycling test up to 100 °C. The difference between the CTE's of the materials is too large, so there will be a large variation in deformation during heating. This difference in expansion leads to the cracks in the braze alloy parallel with the glass-metal interface. In the glass, close to the braze alloy, the maximum principal stress almost reached the value of the ultimate tensile strength at 100 °C in the model with no Ti, but in the Ti model the stress was reduced. So, there should be no problem in the glass. In the corresponding experiment however, small cracks arose in the glass near this location. These cracks can be caused by defects in the glass. Further away from the braze alloy, the stress decreased rapidly in the glass.
Shear stresses occur mainly at the glass-braze transition and in the braze layer the maximum principal stress is also high compared to its maximum strength. So these stresses will limit the strength of the optical viewport. Furthermore, the braze alloy has the lowest ultimate tensile strength. Thus, the braze layer will be the weakest part of the optical viewport. Another braze alloy or other material combinations could reduce the stress in the braze layer and make the viewport stronger.

4. Conclusions

Microstructural analysis has been performed on the glass-metal interface of a brazed fused silica viewport. These SEM analyses were done before and after thermal (cycling) tests of the viewport. We have found that the interlayer near the glass is the weakest part of the joint. The majority of the first cracks occurred in this part after a thermal cycling up to 100 °C. To understand this microstructural behavior, an elastic model of the viewport was developed using the Abaqus code. According to the model the maximum principal stress in the interlayer exceeded the ultimate tensile strength of the braze alloy at a temperature of 100 °C. Moreover, the highest stresses in the interlayer appeared close to the glass. This is the same place as where the microstructural cracks occurred. So the results of our finite element model agree well with our experimental data.

Acknowledgements
The authors are indebted to Mr. S. Huysmans of SCK•CEN for performing the thermal tests. The authors also would like to thank Caburn for the assistance. Viewports are quite expensive, so we were very pleased that Caburn provided us the viewport with small defects for free. These small defects are possibly responsible for the damage observed at temperatures lower than normal (>150 °C).

References
[1] A.E Costley, D.J. Campbell, S. Kasai, K.E. Young and V. Zaveriaev, ITER R&D: Auxiliary Systems: Plasma Diagnostics, Fusion Eng. Des. 55 (2-3) (2001) 331-346
[2] A. Moroño, R. Vila and E.R. Hodgson, KU1 and KS-4V quartz glass lenses for remote handling and diagnostic optical transmission systems, J. Nucl. Mater. 329-333 (2004) 1438-1441
[3] K. Yu. Vukolov, B.A. Levin, Results of irradiation tests of KU-1 and KS-4V silica glasses as ITER candidate window materials, Fusion Eng. Des. 66-68 (2003) 861-864
[4] F. Sato, T. Iida, Y. Oyama, F. Maekawa and Y. Ikeda, Photon emission induced by fusion neutrons on optical window materials, J. Nucl. Mater. 258-263 (1998) 1897-1901
[5] T. Nishitani, T. Shikama, M. Fukao, R. Reichle, T. Sugie, T. Kakuta, S. Kasai, R. Snider and S. Yamamoto, Neutron irradiation tests on diagnostic components at JAERI, Fusion Eng. Des. 56-57 (2001) 905-909
[6] P. Zaccaria and S. Dal Bello, Thermal and mechanical behaviour of diagnostic windows subjected to intense heat fluxes, Fusion Eng. Des. 49-50 (2000) 417-424
[7] M. Lipa, C. Portafaix, E. Pluyette, C. Walker and N. Lochet, Development and testing of diagnostic windows for Tore Supra/CIEL and ITER, Fusion Eng. Des. 61-62 (2002) 801-806
[8] MatWeb, Material property data, www.matweb.com
[9] Solder alloys, www.indium.com
[10] W.C. Jiang, J.M. Gong, S.D. Tu and H. Chen, Three-dimensional numerical simulation of brazed residual stress and its high-temperature redistribution for stainless steel plate-fin structure, Mat. Sci. Eng. A 499 (2009) 293-298
[11] R.L. Williamson, B.H. Rabin and J.T. Drake, Finite element analysis of thermal residual stresses at graded ceramic-metal interface. Part I and II., J. Appl. Phys. 74 (2) (1993) 1310-1326
[12] A. Levy, Thermal residual stresses in ceramic-to-metal brazed joints, J. Am. Ceram. Soc. 74 (9) (1991) 2141-2147
[13] J. Chapa and I. Reimanis, Modeling of thermal stresses in a graded Cu/W joint, J. Nucl. Mater. 303 (2002) 131-136

Figures

Figure 1: Brazed fused silica viewport with 304SS flange.

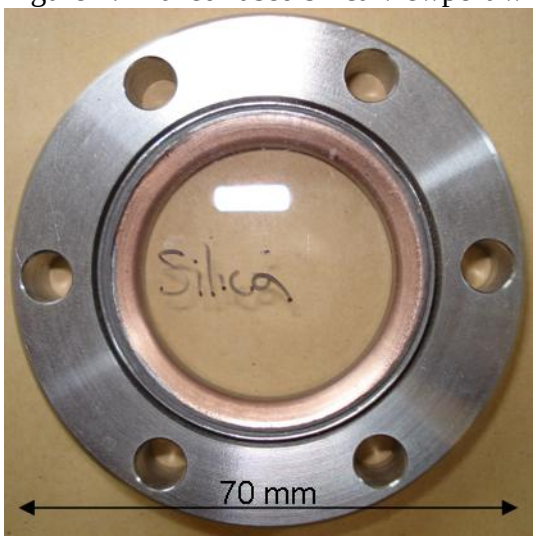

Figure 2: Sample VP cut out of the viewport with the waterjet (left) and the connection of the transparent element to the main stainless steel flange with a 0.3 mm thick holder membrane.

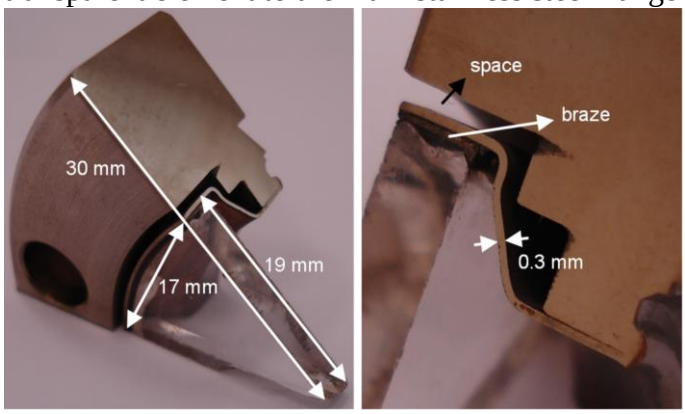

Figure 3: The viewport's geometrical model, the mesh and the paths P1 and P2 along which the stresses were computed.

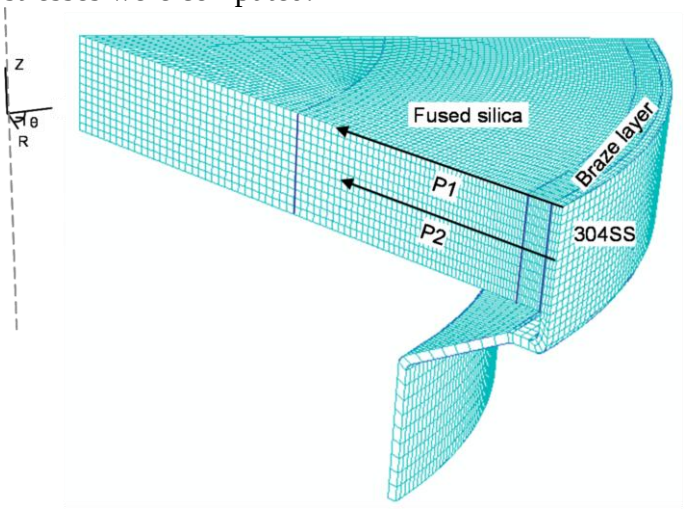

Figure 4: The SEM image of the glass-metal interface of the fused silica viewport shows two interlayers (top left). The Ti is only distributed in the interlayer 2 (top right and bottom left), the Ag is spread out in the whole braze layer (bottom right).

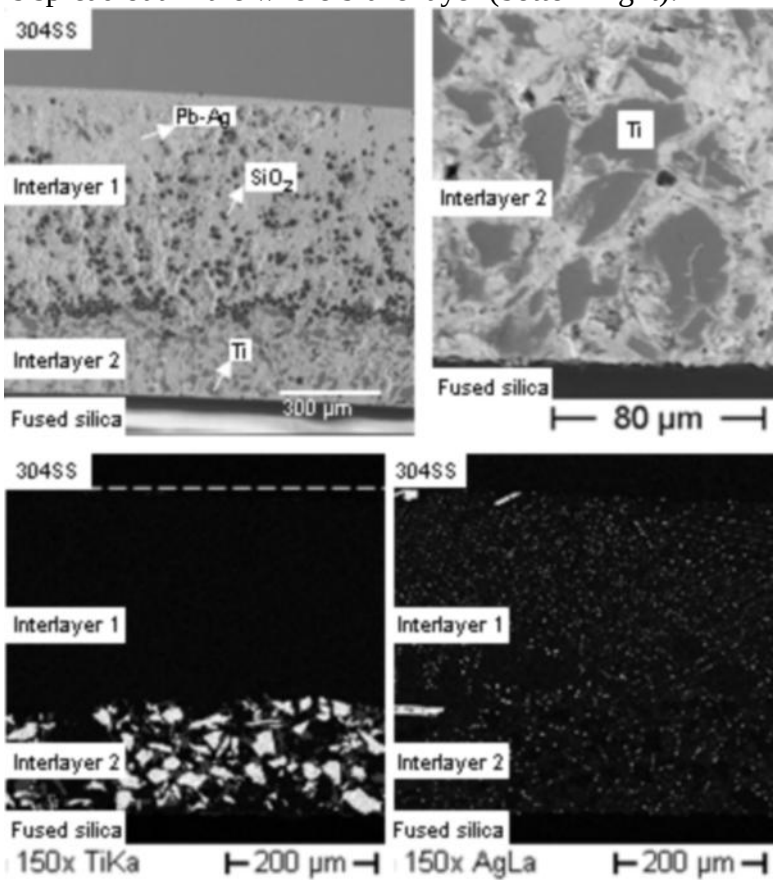

Figure 5: The EDS analysis of the Ti phase in the interlayer.

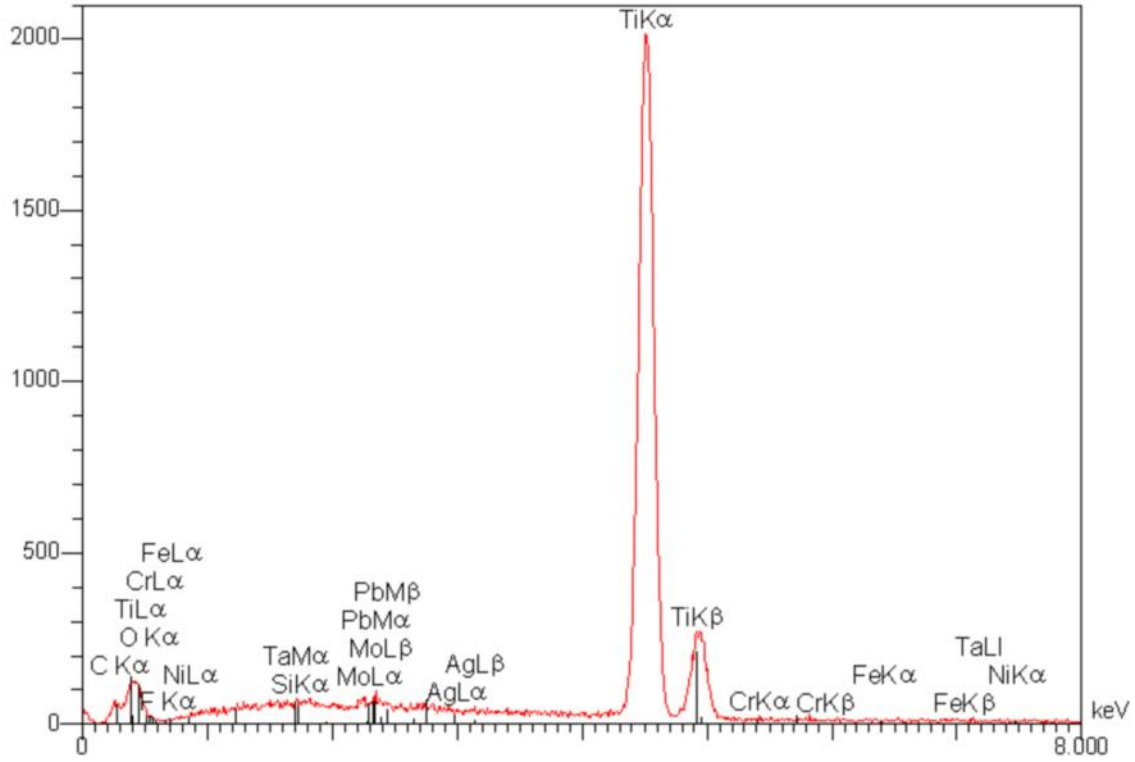

Figure 6: SEM images of the same area of the glass-interlayer 2 interface of the sample VP before tests (A), at 75 °C (B), 100 °C (C), 200 °C (D), 250 °C (E) and 300 °C (F). The white arrows point to the cracks.

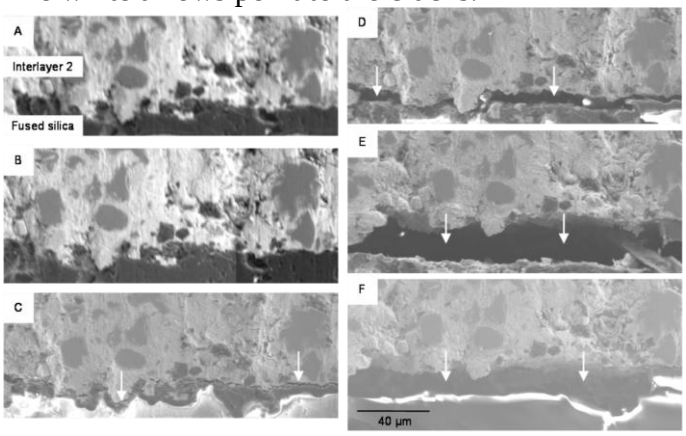

Figure 7: Glass-metal interface of the sample VP at 75 °C (A), 100 °C (B) and 200 °C (C) with a small crack in the glass.

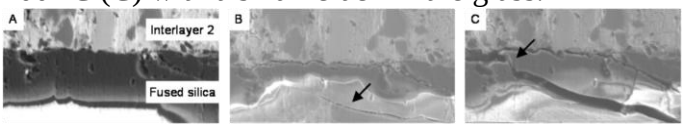

Figure 8: The difference between the interface after the thermal test up to 250 °C (A) and 300 °C (B). The melting of the upper part of the interface is clearly visible.

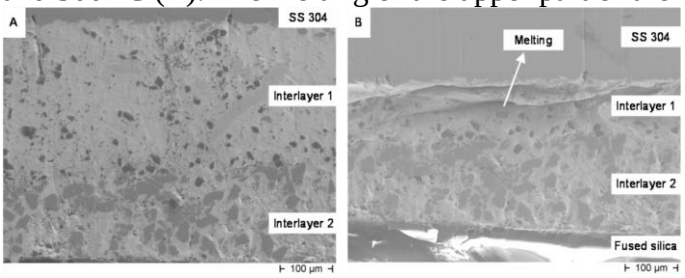

Figure 9: The maximum principal stress at different temperatures in the optical viewport along paths P1 and P2 from the metal to the glass, calculated with the model with no Ti.

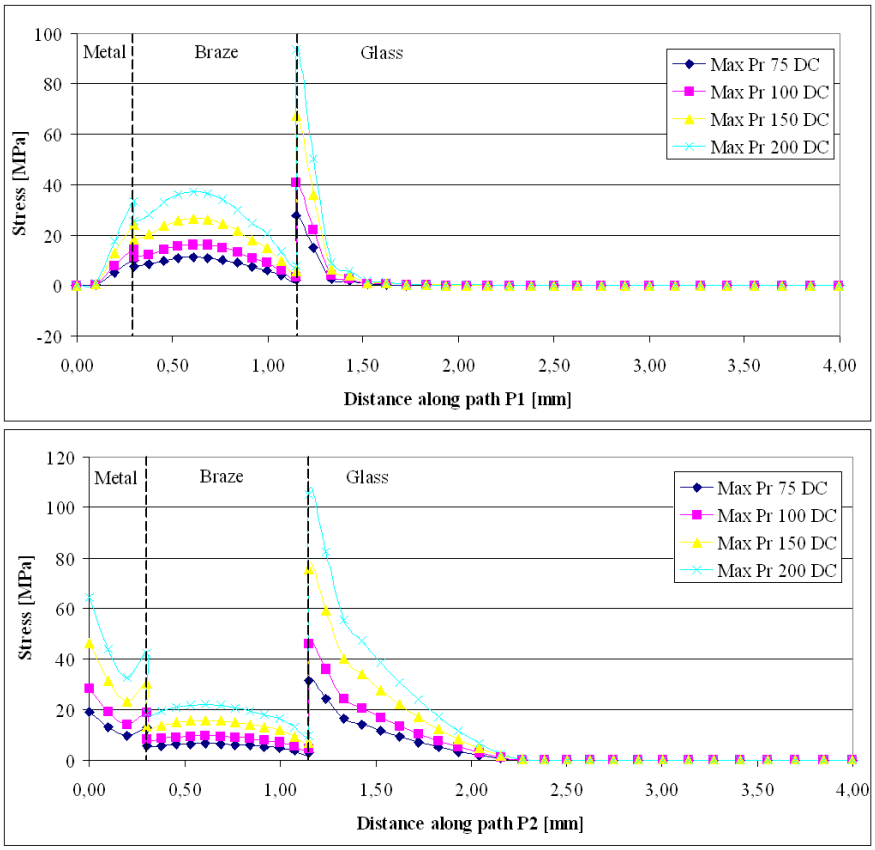

Figure 10: The maximum principal stress at 100 °C in the optical viewport along paths P1 and P2 from the metal to the glass, calculated with the model with no Ti and with 100 % Ti in the interlayer 2 near the glass.

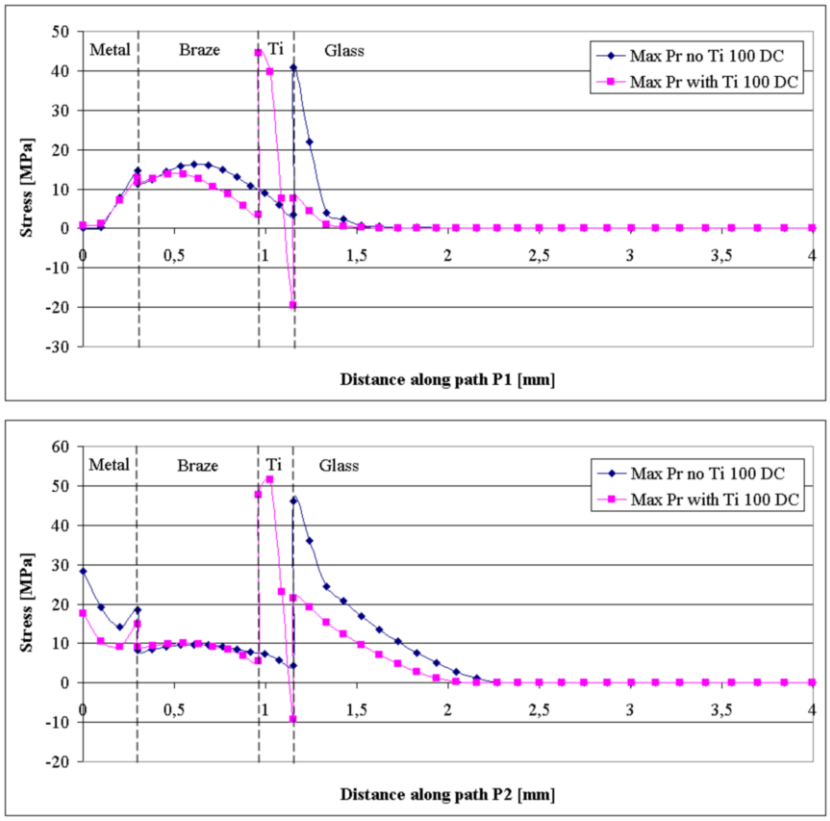

Figure 11: The maximum principal stress at 100 °C for the interface of the viewport with no Ti in the interlayer (left) and with 100 % Ti in interlayer 2 near the glass (right). The maximum principal stress is limited to 50 MPa.

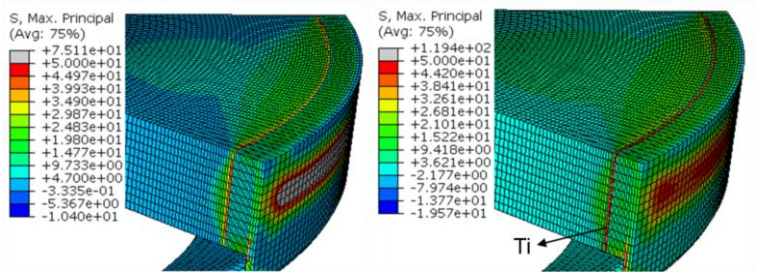

Figure 12: The stresses in each direction σ_{rr} (S11), $\sigma_{\theta\theta}$ (S22) and σ_{zz} (S33), and also the shear stress $\sigma_{r\theta}$ (S12) at 100 °C for the whole sample, calculated with the model with 100 % Ti.

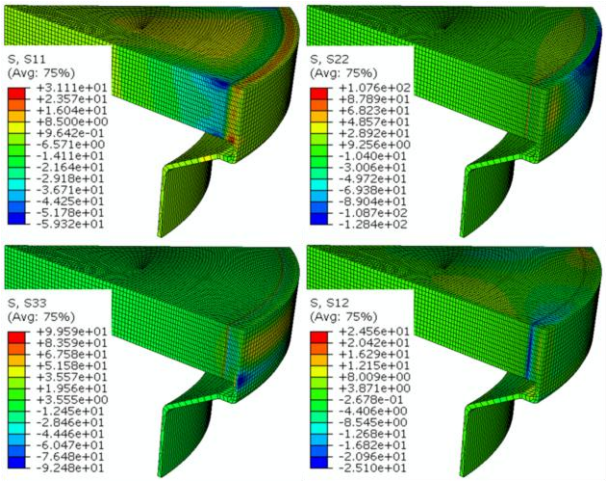

Tables

Table 1: The mechanical material properties of the viewport used in the finite element model

Material	CTE (1/°C)	Young's modulus (GPa)	Poisson's ratio	Yield strength (MPa)	Ultimate tensile strength (MPa)
SiO_2	0.54×10^{-6}	74	0.17	-	50
304SS	17.3×10^{-6}	193	0.29	215	505
Pb-Ag alloy				-	35
92.5Pb 5.0Sn 2.5Ag	29.1×10^{-6}	14	0.42		29
Ti	8.9×10^{-6}	116	0.34	140	220